

Isolation and characterization of synthesis intermediates and side products in hexahydrocannabiphorol

Willi Schirmer^{1,2}  | Ilche Gjuroski² | Martina Vermathen²  | Julien Furrer²  |
Stefan Schürch²  | Wolfgang Weinmann¹ 

¹Institute of Forensic Medicine, Forensic Toxicology and Chemistry, University of Bern, Bern, Switzerland

²Department of Chemistry, Biochemistry and Pharmaceutical Sciences, University of Bern, Bern, Switzerland

Correspondence

Willi Schirmer, Institute of Forensic Medicine, Forensic Toxicology and Chemistry, University of Bern, Murtenstrasse 26, Bern 3008, Switzerland.
Email: willi.schirmer@irm.unibe.ch

Abstract

After the Swiss ban of hexahydrocannabinol (HHC) in March 2023, other semisynthetic dibenzopyran cannabinoids emerged on the Swiss gray market. Hexahydrocannabiphorol (HHCP) was the most prominent of them due to its potent cannabinimimetic effects, as anecdotal reports from recreational users suggest. In October 2023, a class wide ban of dibenzopyran cannabinoids was introduced in Switzerland to prevent new similar substances from entering the drug market. Various vendors in online shops claim that HHCP is made from CBD, even though they possess different alkyl chain lengths. An HHCP sample was analyzed by gas chromatography coupled to mass spectrometry (GC-MS), showing that a mixture of molecules with the same or a similar molecular mass as HHCP was present. Six different substances could be isolated from this sample using column chromatography. Four phenols ((9*R*)-HHCP, *iso*-HHCP, *cis*-HHCP, and *abn*-HHCP) and two ketones (possible intermediates to (9*R*)-HHCP and *abn*-HHCP) were identified by various nuclear magnetic resonance spectroscopy (NMR) techniques. (9*S*)-HHCP was obtained in an impure fraction. In addition, a fraction was obtained that showed characteristic molecular and fragment ions consistent with bisalkylated products from the synthesis of similar compounds. The presence of abnormal cannabinoids (*abn*-HHCP) and bisalkylated cannabinoids is a confirmation that this sample was produced purely synthetically as initially suspected, as these compounds have not been reported in *Cannabis*. Chiral derivatization of the phenols with Mosher acid chlorides showed that only *iso*-HHCP was present as a scalemic mixture, indicating a good stereocontrol of this synthetic procedure.

KEYWORDS

cannabis, hexahydrocannabinol (HHC), hexahydrocannabiphorol (HHCP), isomeric cannabinoids, Mosher ester

1 | INTRODUCTION

Hexahydrocannabiphorol (HHCP, also named HHCp, HHC-P, or HHC-C7) is a synthetic cannabinoid with a dibenzopyran structure like

tetrahydrocannabinol (THC). Like hexahydrocannabinol (HHC) before it was banned, HHCP was also sold as a legal alternative to THC in Switzerland. On October 9, 2023, Switzerland issued a group-wide ban on cannabinoids with a dibenzopyran structure, placing HHCP

This is an open access article under the terms of the [Creative Commons Attribution-NonCommercial](https://creativecommons.org/licenses/by-nc/4.0/) License, which permits use, distribution and reproduction in any medium, provided the original work is properly cited and is not used for commercial purposes.

© 2024 The Author(s). *Drug Testing and Analysis* published by John Wiley & Sons Ltd.

and structurally similar compounds under control. This was in response to the legal dibenzopyran-cannabimimetics emerging on the gray market after the ban of HHC on March 31, 2023.¹

The aim of this work was to identify stereoisomers, synthesis side products, precursors, or the absolute configuration of the HHCP epimers in a product obtained from a German vendor to get an insight about the HHCP on the market. The claim that HHCP and similar dibenzopyran cannabinoids are synthesized from CBD with an alkyl side chain other than pentyl should be verifiable. A synthetic route from CBD is unlikely, as it involves a homologation step of a pentyl chain without functional groups. Synthetic approaches for dibenzopyran cannabinoids from the literature start with a 5-alkylresorcinol or a 5-alkylcyclohexane-1,3-dione with the desired chain length. It is also possible to isolate Δ^9 -tetrahydrocannabiphorol (THCP), a minor cannabinoid, from a *Cannabis* strain with higher THCP content and hydrogenate that fraction to obtain HHCP. This, however, is unlikely since the THCP content is still very low, making the process very costly.² To the authors' knowledge, neither the potency nor the affinity of HHCP towards the human cannabinoid receptor 1 (hCB₁) is known yet, but anecdotal reports from users suggest that it is more potent than THC. Concerning THCP, it is known that the affinity towards hCB₁ in vitro is 30 times higher than for THC.³

2 | MATERIALS AND METHODS

2.1 | Chemicals and reagents

The HHCP sample was bought from an online shop in Germany (52% (9R)-HHCP and 21% (9S)-HHCP, gas chromatography coupled to mass spectrometry (GC-MS) area-% (not quantified)). *N*-methyl-*N*-trimethylsilyltrifluoroacetamide (MSTFA) ($\geq 98.5\%$), 4-(dimethylamino)pyridine (DMAP) ($\geq 99\%$), (*R*)-(-)- α -Methoxy- α -(trifluoromethyl)-phenylacetyl chloride ((*R*)-MTPA-Cl), (*S*)-(+)- α -Methoxy- α -(trifluoromethyl)-phenylacetyl chloride ((*S*)-MTPA-Cl), and the alkane standard (C7-C40, 1,000 $\mu\text{g}/\text{ml}$) were purchased from Sigma-Aldrich (Buchs, Switzerland). (9R)-HHCP, (9S)-HHCP, cannabidiphorol (CBDP), and cannabiphorol (CBP) were purchased from Cayman Chemical (Ann Arbor, United States). Ethyl acetate (EtOAc) (for liquid chromatography), *n*-hexane (for analysis), Na₂SO₄ sicc. (for analysis, Reag. Ph. Eur.), and dichloromethane (DCM) (for analysis, Reag. Ph. Eur.) were from Grogg Chemie (Stettlen, Switzerland). Methanol (MeOH) ($\geq 99.9\%$) was from Carl Roth (Karlsruhe, Germany). Silica gel 60 (0.015–0.04 mm) from Macherey-Nagel (Önsingen, Switzerland) was used. Deuterated chloroform, CDCl₃ (99.80% D), was purchased from Eurisotop (St.-Aubin Cedex, France) and used as solvent for the nuclear magnetic resonance spectroscopy (NMR) measurements.

2.2 | Chiral derivatization solutions

(*S*)-MTPA-Cl or (*R*)-MTPA-Cl (5 μl) was diluted with 495 μl dry DCM. The solution was kept over Na₂SO₄ sicc.

2.3 | DMAP solution

DMAP (10 mg) was dissolved in 1 ml dry DCM. The solution was kept over Na₂SO₄ sicc.

2.4 | Column chromatographic separation

A part of the HHCP sample (250 mg) was separated on silica gel starting from *n*-hexane: EtOAc (100:1, V:V) as eluent.⁴ The polarity of the eluent was stepwise increased to pure EtOAc. Collected fractions were analyzed by GC-MS. Pure fractions containing the same product were unified and evaporated to dryness.

2.5 | GC-MS analysis

The isolated samples were analyzed using an 8890 gas chromatograph with a 7693A autosampler coupled to a 5977B mass selective detector (Agilent, Basel, Switzerland). Data were acquired with MassHunter Workstation GC/MS Data Acquisition (Version 10.1.49) and analyzed with Enhanced ChemStation (F.01.03.2357) (Agilent). Chromatography was performed on a 5% phenylmethylsiloxane column (HP-5 ms Ultra Inert, 30 m, 250 μm i.d., 0.25 μm film thickness; Agilent J&W). Helium was used as a carrier gas with a constant flow of 1 ml/min. The injection volume was 1 μl in pulsed splitless mode. Oven temperature started at 70°C for 3 min and was ramped with 15°C/min to 290°C and held for 19 min, resulting in a total separation time of 36.7 min. The source temperature was set to 230°C, and the quadrupole temperature was 150°C. EI mass spectra were obtained with an ionization energy of 70 eV. Depending on the experiment, the scan range was set from *m/z* 35 to 450, from *m/z* 35 to 650, or from *m/z* 35 to 800.

2.6 | NMR analysis

The NMR spectra were recorded on Bruker Avance II and Avance NEO spectrometers operating at resonance frequencies of 400.33 and 500.13 MHz for ¹H nuclei and 100.66 and 125.76 MHz for ¹³C nuclei, respectively (Bruker BioSpin AG, Fällanden, Switzerland). The instruments are equipped with a 5 mm dual (¹H/¹³C) probe (400 MHz) and a 1.7 mm triple (¹H/¹³C/³¹P) TXI microprobe (500 MHz) both with z-gradient coils. All measurements were carried out at room temperature (*T* = 298 K). Acquisition and processing of the spectra were done using the Bruker software TopSpin versions 4.1.4 and 4.0.9. ¹H chemical shifts were referenced to the residual ¹H resonance of CDCl₃ ($\delta^1\text{H} = 7.264$ ppm), and ¹³C chemical shifts were referenced through the ¹³C resonance of CDCl₃ (set to $\delta^{13}\text{C} = 77.5$ ppm).

One- and two-dimensional NMR experiments were performed using the Bruker pulse program library (the names of pulse programs are given in brackets). 1D proton spectra were acquired using the standard one-pulse experiment with a 30° flip angle (zg30). For structure elucidation, the following 2D experiments were applied: ¹H-¹H-

COSY using magnitude mode with gradients and purge pulses (*cosygpppqf*), ^1H - ^{13}C -HSQC with carbon multiplicity editing and echo-antiecho acquisition mode (*hsqcedetgpsisp2.3*), ^1H - ^{13}C -HMBC with low-pass J-filter to suppress one-bond correlations and magnitude acquisition mode (*hmbclpndqf*), and ^1H - ^1H -NOESY in phase sensitive mode using a mixing time of 300 ms (*noesygpphpp*).

^1H and ^{13}C chemical shift prediction was performed using the ChemDraw software, version 20.0.0.41 (PerkinElmer Informatics, Inc.), and used to support resonance assignments.

3 | RESULTS AND DISCUSSION

3.1 | Purity of the sample

The HHCP sample was diluted to 100 mg/L and analyzed by GC-MS. Besides (9*R*)-HHCP and (9*S*)-HHCP, several substances were detected with the same molecular ion of m/z 344 and the same fragment ions, indicating the presence of isomers. Other compounds in the sample showed a molecular ion of m/z 346. The total ion current chromatogram of a sample solution is shown in Figure 1. The absence of palmitic acid and stearic acid is a hint that no plant extract might have been used for the synthesis. Unpublished casework showed that these fatty acids are present in HHC samples deriving from natural CBD. A fraction with Kováts indices of 2,900–3,400 was collected. This fraction contained numerous compounds with molecular ions of

m/z 480 and 482. XIC of the fragment ion m/z 395 from the HHCP sample is included in Supporting Information S104.

3.2 | Identification of components by NMR

Six different components were isolated by column chromatography including (9*R*)-HHCP. They are shown in Figure 2. Structural elucidation was determined using various NMR-experiments. The isolated compounds are described in order of column chromatographic elution; the NMR spectra are found in Supporting Information S1–S58.

3.2.1 | Structure elucidation of compound 1

^1H -NMR revealed two aromatic protons in *meta*-orientation (H-8 and H-10) and a phenolic proton. The methyl groups appear as a singlet (H-12), two doublets (H-14 and H-15), and a triplet (H-7'), which is different to the methyl groups of HHCP, as they appear as two singlets, a doublet, and a triplet. This indicates another structure of the terpenoid moiety than in HHCP. The correlations in the 2D-NMR spectra indicate an *iso*-propyl group (COSY cross peak between H-13 and H-14, 15) and a bicyclic structure. HMBC correlates the bridged carbon at position C5 to both *iso*-propyl CH_3 -protons (H-15/C-5 and H-14/C-5). In addition, NOE cross peaks are detected between H-5 and H-15, H-6 and H-15, H-11, and between H-4 and H-14.

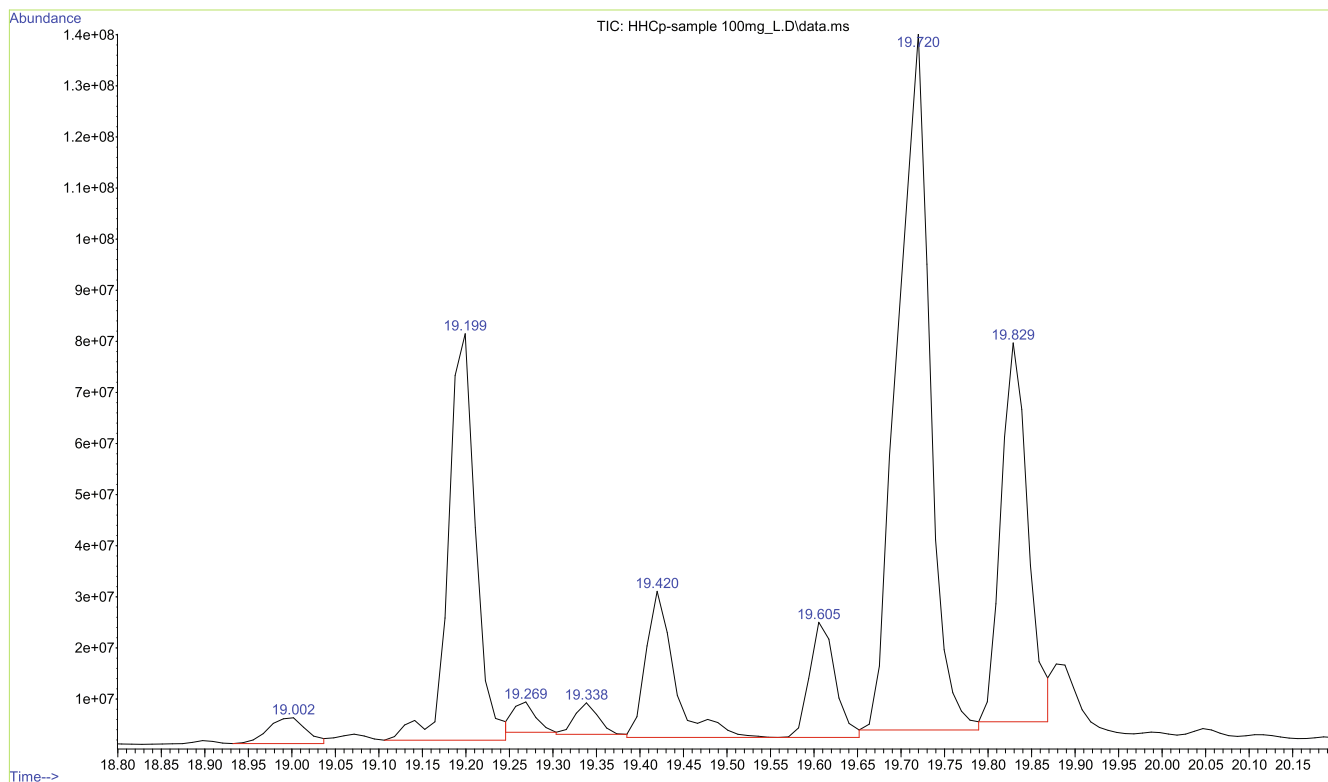


FIGURE 1 TIC of the HHCP sample ($\gamma = 100$ mg/L). Other compounds besides the isolated compounds 1–6 are present.

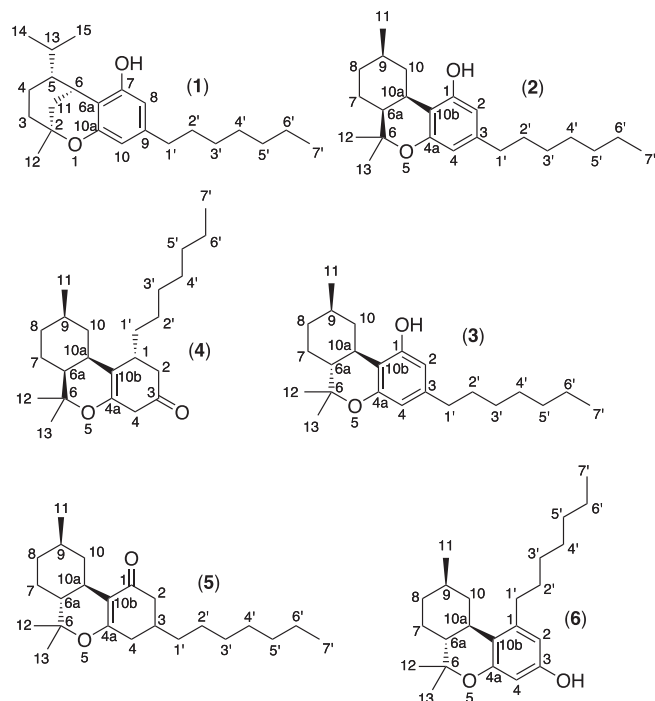


FIGURE 2 Isolated compounds *iso*-HHCP (**1**), *cis*-(9*R*)-HHCP (**2**), (9*R*)-HHCP (**3**), precursor to *cis*-*abn*-HHCP (**4**), precursor to (9*R*)-HHCP (**5**), and *abn*-HHCP (**6**).

H-5 and H-6 only yield weak NOE. This leads to the structure of *rel*-(2*S*,5*R*,6*S*)-9-heptyl-5-isopropyl-2-methyl-3,4,5,6-tetrahydro-2*H*-2,6-methanobenzo[*b*]oxocin-7-ol (*iso*-HHCP, dihydro-*iso*-THCP). The protons (H-14 and H-15) of the *iso*-propyl group are diastereotopic due to the chiral centers. The non-equivalency of methyl shifts in branched, chiral *iso*-propyl moieties has been reported in the literature.^{5,6} The pentyl-homolog of compound **1**, *iso*-HHC, shows the same non-equivalency of these particular methyl groups.^{4,6-9} The ¹H and ¹³C resonance assignments are summarized in Table 1. The NMR spectra of compound **1** are found in Supporting Information S1–S12.

3.2.2 | Structure elucidation of compounds **2** and **3**

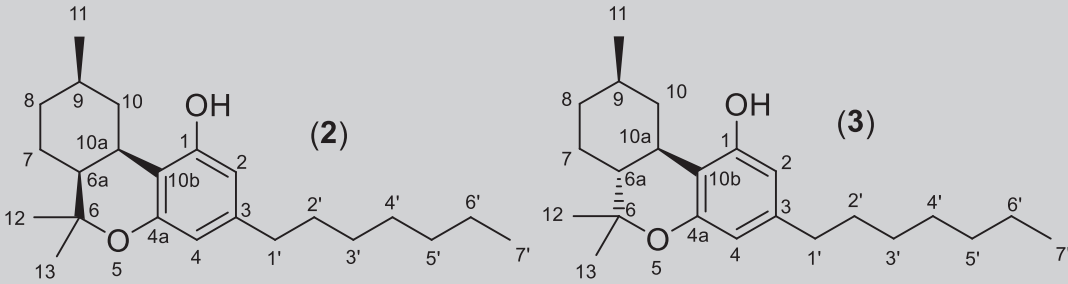
In the ¹H-NMR spectrum of compound **2**, two aromatic protons (H-2' and H-4') in *meta*-position could be identified. In addition, four methyl groups were identified appearing as a doublet (H-11), two singlets (H-12 and H-13), and a triplet (H-7') as in (9*R*)-HHCP. Correlations in the 2D-spectra indicated a constitution like in HHCP. The shifts are very similar to (9*R*)-HHCP but change notably in proximity of the stereogenic centers. NOESY spectrum indicates that the stereochemistry at C10a differs from (9*R*)-HHCP; a cross peak correlates proton H-10a to proton H-9; a *trans*-diaxial orientation of these two protons might be the reason. The protons (H-10a and H-6a) are correlated by NOESY, indicating a *cis*-configuration of this compound. Compound

TABLE 1 ¹³C- and ¹H shifts of *iso*-HHCP (**1**) in CDCl₃.

Nr.	$\delta(^{13}\text{C})/\text{ppm}$	$\delta(^1\text{H})/\text{ppm}$
Phenolic H	-	4.49 (s, br 1H)
1	-	-
2	74.8	-
3	41.0	1.98 (m, 1H) 1.48 (m, 1H)
4	23.6	1.06 (ddd, $J = 12.9, 4.4$ Hz, 1H) 1.59 (td, $J = 13.2, 4.9$ Hz, 1H)
5	51.3	1.26 (m, 1H)
6	30.3	3.40 (dt, $J = 3.5$ Hz, 2.5 Hz 1H)
6a	109.4	-
7	153.9	-
8	106.9	6.09 (d, $J = 1.5$ Hz, 1H)
9	143.4	-
10	108.9	6.26 (d, $J = 1.4$ Hz, 1H)
10a	158.5	-
11	38.5	1.78 (m, 2H)
12	29.6	1.34 (s, 3H)
13	30.3	1.40 (m, 1H)
14	21.6	0.75 (d, $J = 6.6$ Hz, 3H)
15	23.8	1.12 (d, $J = 6.3$ Hz, 3H)
1'	36.6	2.45 (m, 2H)
2'	31.8	1.57 (m, 2H)
3'	30.3	1.30 (m, 2H)
4'	30.4	1.26 (m, 2H)
5'	32.7	1.27 (m, 2H)
6'	23.5	1.29 (m, 2H)
7'	15.2	0.88 (m, 3H)

2 was identified as *rel*-(6*aS*,9*R*,10*aR*)-3-heptyl-6,6,9-trimethyl-6*a*,7,8,9,10,10*a*-hexahydro-6*H*-benzo[*c*]chromen-1-ol (*cis*-HHCP). The NMR spectra of compound **2** are found in Supporting Information S13–S23.

Compound **3** is (9*R*)-HHCP; this was confirmed by GC-MS using a reference standard. The ¹H- and ¹³C-NMR shifts of this compound are in accordance to the literature.⁴ The ¹H and ¹³C resonances of compounds **2** and **3** are summarized in Table 2. The NMR spectra of compound **3** are found in Supporting Information S24–S28.

TABLE 2 ^{13}C - and ^1H shifts of *cis*-(9*R*)-HHCP (**2**) and (9*R*)-HHCP (**3**) in CDCl_3 .


Nr.	<i>cis</i> -HHCP (2)		(9 <i>R</i>)-HHCP (3)	
	$\delta(^{13}\text{C})/\text{ppm}$	$\delta(^1\text{H})/\text{ppm}$	$\delta(^{13}\text{C})/\text{ppm}$	$\delta(^1\text{H})/\text{ppm}$
Phenolic H	-	4.65 (s, 1H)	-	5.88 (m, 1H)
1	156.6	-	155.1	-
2	110.5	6.25 (d, $J = 1.8$ Hz, 1H)	110.1	6.31 (d, $J = 1.8$ Hz, 1H)
3	143.0	-	142.8	-
4	108.6	6.06 (d, $J = 1.8$ Hz, 1H)	108.3	6.11 (d, $J = 1.8$ Hz, 1H)
4a	156.6	-	156.7	-
5	-	-	-	-
6	76.9	-	77.6	-
6a	42.8	1.49 (ddd, $J = 9.0, 5.3, 4.1$ Hz, 1H)	49.6	1.51 (m, 1H)
7	23.9	1.27 (m, 1H) 1.78 (m, 1H)	28.4	1.14 (m, 1H) 1.87 (m, 1H)
8	35.9	0.94 (m, 1H) 1.65 (ddt, $J = 12.8, 6.7, 3.1$ Hz, 1H)	36.0	1.11 (m, 1H) 1.89 (m, 1H)
9	27.9	1.19 (m, 1H)	33.2	1.66 (m, 1H)
10	38.2	1.09 (m, 1H) 3.13 (dq, $J = 13.2, 2.6$ Hz, 1H)	39.3	0.82 (m, 1H) 3.17 (dt, $J = 13.0, 3.2$ Hz, 1H)
10a	32.0	3.27 (ddd, $J = 4.3, 4.3, 4.3$ Hz, 1H)	35.8	2.53 (td, $J = 11.1, 2.9$ Hz, 1H)
10b	108.6	-	110.9	-
11	23.1	0.84 (d, $J = 6.5$ Hz, 3H)	22.9	0.99 (d, $J = 6.6$ Hz, 3H)
12	26.1	1.23 (s, 3H)	19.3	1.10 (s, 3H)
13	27.2	1.36 (s, 3H)	28.0	1.43 (s, 3H)
1'	36.2	2.43 (dd, $J = 9.0, 6.7$ Hz, 2H)	35.8	2.44 second order
2'	31.7	1.56 second order	31.3	1.56 (m, 2H)
3'	30.2	1.27 (m, 2H)	29.7	1.33 (m, 2H)
4'	30.2	1.29 (m, 2H)	29.7	1.33 (m, 2H)
5'	32.4	1.29 (m, 2H)	32.2	1.32 (m, 2H)
6'	23.9	1.27 (m, 2H)	22.9	1.32 (m, 2H)
7'	14.9	0.88 (t, $J = 7.2$ Hz, 3H)	14.5	0.93 (t, $J = 7.0$ Hz, 3H)

3.2.3 | Structure elucidation of compounds **4** and **5**

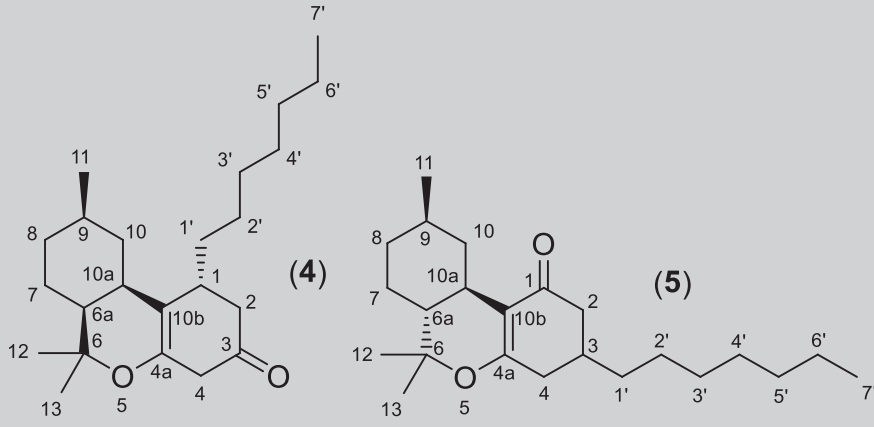
Compound **4** showed no aromatic or olefinic protons in the ^1H -NMR. HMBC revealed the presence of a ketone and an olefin. Since no olefinic protons were found, a tetrasubstituted olefin was concluded. The four methyl groups consist of two singlets (H-12 and H-13), a doublet (H-11), and a triplet (H-7') like in HHCP. Further correlations

in the 2D-NMR spectra lead to a dibenzopyran structure like in HHCP. The COSY correlation (H-1 and H-1') and the HMBC correlations (H-2 and C-3, H-4, and C-3) indicate that the positions of the substituents at C-1 and C-3 are exchanged in comparison to (9*R*)-HHCP. NOESY crosspeaks were found between H-10a and H-11, indicating a *trans*-diaxial relation between them, and a correlation between H-10a and H-6a, indicating a *cis*-relation between the

respective carbons C-10a and C-6a. No NOESY crosspeak was detected between H-1' and H-10, indicating the same configuration at the atoms C-10a and C-1'. The opposite configuration on these

two carbons should lead to shorter distances between the attached hydrogens and therefore to a positive NOESY correlation. The correlations lead to the structure of *rel*-(1*R*,6*aS*,9*R*,10*aR*)-1-heptyl-

TABLE 3 ^{13}C - and ^1H shifts of the ketones **4** and **5** in CDCl_3 .



Nr.	Compound 4		Compound 5	
	$\delta(^{13}\text{C})/\text{ppm}$	$\delta(^1\text{H})/\text{ppm}$	$\delta(^{13}\text{C})/\text{ppm}$	$\delta(^1\text{H})/\text{ppm}$
1	33.6	2.07 (m, 1H)	199.6	-
2	44.4	2.26 (m, 1H) 2.43 (dd, $J = 15.8, 4.7$ Hz, 1H)	44.8	2.22 (m, 1H) 2.47 (m, 1H)
3	199.7	-	33.3	1.55(m, 1H)
4	36.0	2.23 (m, 1H) 2.35 (m, 1H)	36.3	2.24 (m, 1H) 2.32 (m, 1H)
4a	171.3	-	171.1	-
5	-	-	-	-
6	80.2	-	81.8	-
6a	41.6	1.43 (ddd, $J = 12, 5, 5$ Hz, 1H)	49.4	1.23 (m, 1H)
7	23.3	1.0 (m, 1H) 1.71 (m, 1H)	28.1	1.04 (m, 1H) 1.73 (m, 1H)
8	35.0	0.85 (m, 1H) 1.65 (m, 1H)	36.3	1.00 (m, 1H) 1.81 (m, 1H)
9	20.6	1.03 (m, 1H)	26.4	1.20 (m, 1H)
10	36.1	0.91 (m, 1H) 2.95 (dd, $J = 13.4, 2.8$ Hz, 1H)	39.0	0.45 (q, $J = 11.7$ Hz, 1H) 2.84 (dq, $J = 12.8, 3.4$ Hz, 1H)
10a	29.9	2.85 (m, 1H)	34.3	2.07 (m, 1H)
10b	111.2	-	114.9	-
11	22.9	0.81 (d, $J = 6.4$ Hz, 3H)	23.1	0.90 (d, $J = 7.2$ Hz, 3H)
12	26.1	1.20 (s, 3H)	20.6	1.06 (s, 3H)
13	26.4	1.31 (s, 3H)	28.0	1.34 (s, 3H)
1'	35.4	1.36 (m, 2H)	35.8	1.37 (m, 2H)
2'	27.2	1.28 (m, 2H)	29.9	1.27 (m, 2H)
3'	30.0	1.25 (m, 2H)	27.8	1.27 (m, 2H)
4'	30.0	1.26 (m, 2H)	27.6	1.27 (m, 2H)
5'	32.5	1.27 (m, 2H)	32.5	1.26 (m, 2H)
6'	23.0	1.29 (m, 2H)	23.2	1.28 (m, 2H)
7'	14.6	0.88 (t, $J = 7.0$ Hz, 3H)	14.7	0.88 (t, $J = 6.5$ Hz, 3H)

6,6,9-trimethyl-2,3,4,6,6a,7,8,9,10,10a-decahydro-1*H*-benzo[*c*]chromen-3-one. The NMR spectra of compound **4** are found in Supporting Information S29–S37.

¹H-NMR of compound **5** showed that this compound does not contain any aromatic or olefinic protons. HMBC signals in the lower field can be seen indicating an olefin and a ketone. Considering the dibenzopyran structure of HHCP, it was assumed that the oxo group is located where the phenol would otherwise be found. The olefin is located where the aromatic and heterocyclic rings are fused, resulting in a tetrasubstituted olefin. Two singlets (H-12 and H-13) on similar positions like in the ¹H-NMR spectrum of (9*R*)-HHCP are present, which are likely the geminal methyl groups. The other methyl groups are overlaid around 0.9 ppm. Spin-spin-multiplicity (doublet H11 and triplet H7') indicates that they are bound to a R₂CH group and a RCH₂ group, respectively, like in HHCP. The correlations in the 2D-NMR lead to the structure of *rel*-(6*aR*,9*R*,10*aR*)-3-heptyl-6,6,9-trimethyl-2,3,4,6,6a,7,8,9,10,10a-decahydro-1*H*-benzo[*c*]chromen-1-one. No NOESY crosspeak was found between H-10a and H-6a, indicating a *trans*-configuration. No crosspeak was found between H-10a and H-11 but one between H-10a and H-9. Stereochemistry at position C-3 could not be determined. The ¹H and ¹³C resonances of compounds **4** and **5** are summarized in Table 3. NMR spectra of compound **5** are found in Supporting Information S38–S44.

3.2.4 | Structure elucidation of compound **6**

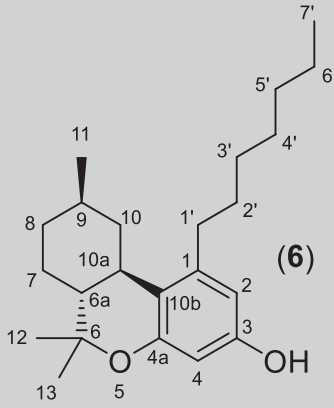
¹H-NMR revealed the presence of two aromatic protons with the same multiplicities and coupling constant as in HHCP indicating *meta*-orientation of the protons. Multiplicity of the methyl groups is the same as in HHCP (two singlets [H-12 and H-13], a doublet [H-11], and a triplet [H-7']); these signals were assigned to the same methyl groups. The correlations in the 2D-NMR spectra indicate that the positions of the heptyl-group and the phenol are exchanged. A correlation between protons H-1 and H-1' and between H-1 and H-10b are seen in the HMBC spectrum. NOESY shows that H-1' of the heptyl chain and H-10 are in close proximity confirming that structure. Protons H-11 and the proton at H-10a show a NOESY crosspeak indicating *trans*-diaxial orientation of these two protons. The missing crosspeak between protons H-10a and H-6a indicates a *trans*-configuration of the molecule leading to the molecule *rel*-(6*aR*,9*R*,10*aR*)-1-heptyl-6,6,9-trimethyl-6a,7,8,9,10,10a-hexahydro-6*H*-benzo[*c*]chromen-3-ol. ¹H-NMR spectrum looks similar to the homolog *cis*-*abn*-HHC.¹⁰ The ¹H and ¹³C resonances of compound **6** are summarized in Table 4. NMR spectra of compound **6** are found in Supporting Information S45–S58.

3.3 | Mass spectrometric elucidation

3.3.1 | Formation of HHCP mass fragments

The mass spectra of (9*R*)-HHCP and (9*S*)-HHCP are indistinguishable. Figure 3 shows the mass spectrum of (9*R*)-HHCP. Their major ions are

TABLE 4 ¹³C- and ¹H shifts of *abn*-HHCP (**6**) in CDCl₃.



Compound 6		
Nr.	δ(¹³ C)/ppm	δ(¹ H)/ppm
Phenolic H	-	4.31 (very broad)
1	143.8	-
2	109.1	6.27 (d, <i>J</i> = 2.6 Hz, 1H)
3	154.9	-
4	102.1	6.14 (d, <i>J</i> = 2.7 Hz, 1H)
4a	155.3	-
5	-	-
6	76.6	-
6a	51.4	1.52 (m, 1H)
7	32.1	1.30 (m, 1H) 1.65 (m, 1H)
8	23.8	1.53 (m, 1H) 1.68 (m, 1H)
9	28.3	2.13 (dtd, <i>J</i> = 7.3, 4.7, 2.4 Hz, 1H)
10	39.4	1.38 (m, 1H) 2.22 (m, 1H)
10a	30.9	2.65 (td, <i>J</i> = 11.2, 2.6 Hz, 1H)
10b	117.5	-
11	18.6	1.16 (d, <i>J</i> = 7.2 Hz, 3H)
12	27.5	1.05 (s, 3H)
13	18.5	1.36 (s, 3H)
1'	33.5	2.55 (ddd, <i>J</i> = 9.6, 7.0, 2.8 Hz, 2H)
2'	31.3	1.60 (m, 2H)
3'	29.6	1.33 (m, 2H)
4'	29.6	1.33 (m, 2H)
5'	22.8	1.31 (m, 2H)
6'	22.8	1.31 (m, 2H)
7'	14.1	0.90 (t, <i>J</i> = 6.7 Hz, 3H)

the molecular ion (*m/z* 344), loss of a propyl radical from the *gem*-dimethyl group ([M-C₃H₇]⁺, *m/z* 301), loss of *n*-hexene from the side chain after McLafferty rearrangement ([M-C₆H₁₂]⁺, *m/z* 260, base peak), and the tropylium ion ([M-123]⁺, *m/z* 221). Some minor ions like the loss of a methyl radical ([M-CH₃]⁺, *m/z* 329) and the ion *m/z*

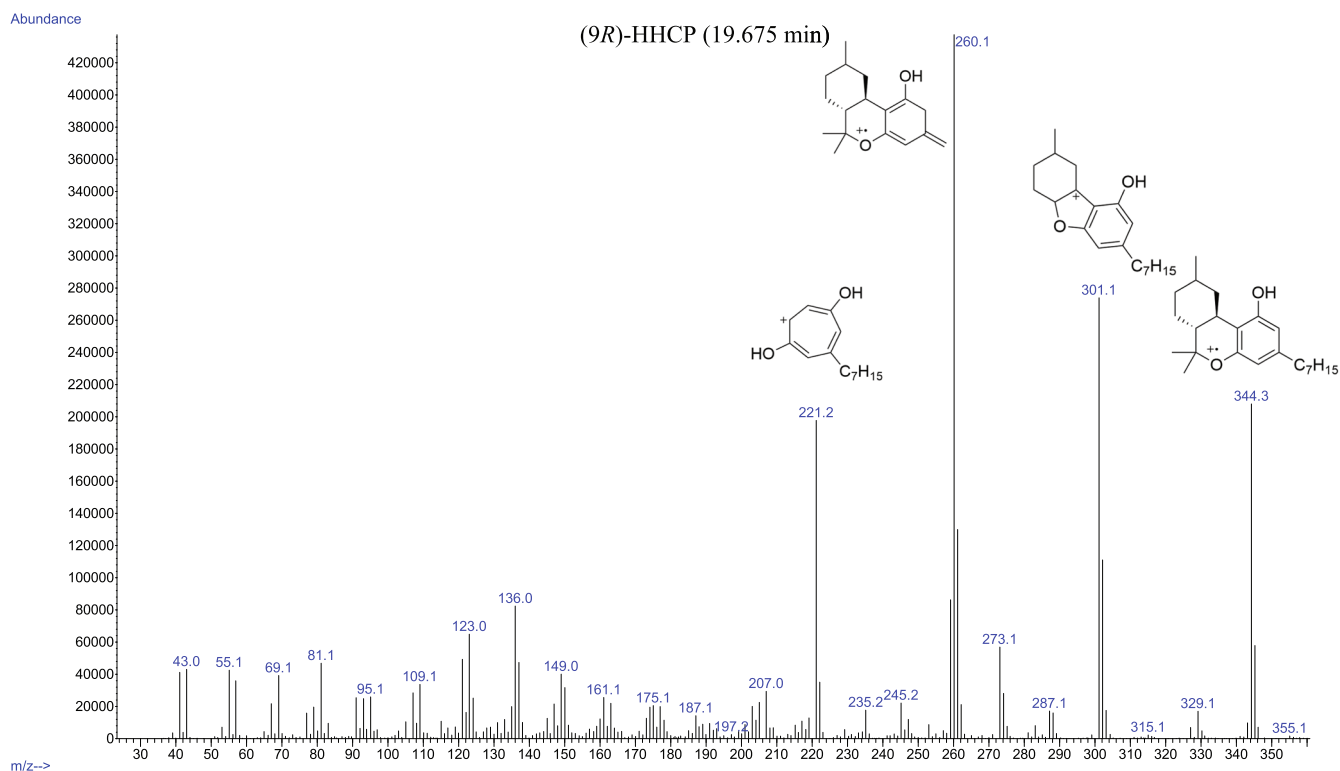


FIGURE 3 Mass spectrum of (9R)-HHCP with the structures of the most abundant ions.

136 from the alicyclic moiety are also visible. The fragmentation mechanisms are in analogy to other well characterized cannabinoids.^{11–13}

An alkane standard (C7–C40) was measured, and the Kováts index¹⁴ of the isolated compounds and the references were calculated according to van den Dool and Kratz.¹⁵ The data are summarized in Table 5. A chromatogram of the alkane standard is included in Supporting Information S59.

3.3.2 | Mass spectrum of compound 1

The mass spectrum of compound 1 consists of only a few ions with high intensity: the molecular ion ($[M]^+$, m/z 344), loss of *n*-hexene from the side chain ($[M-C_6H_{12}]^+$, m/z 260), and loss of a *iso*-hexyl radical ($[M-C_6H_{13}]^+$, m/z 259, base peak).¹⁶ Other fragments with lower abundance like the tropylium ion at m/z 221 and loss of a methyl radical at m/z 329 are also present. Mass spectrum is similar to the pentyl analog *iso*-HHC described in literature. The ions m/z 221, 301, and 344 are shifted by +28 (ethylene) in comparison to the ions of *iso*-HHC. The ion m/z 260, which results from the McLafferty rearrangement, is the same.⁴

3.3.3 | Mass spectrum of compound 2

This compound shows the same fragments with the same abundances as (9R)-HHCP and (9S)-HHCP. NMR data imply a *cis*-

TABLE 5 Chromatographic data and relevant ions of the isolated compounds and reference compounds.

Name	RT/min	RRI	Relevant ions
Compound 1	19.12	2,615	344, 260, 259, 221
Compound 2	19.18	2,623	344, 301, 260, 221
Compound 3	19.68	2,692	344, 301, 260, 221
Compound 4	18.62	2,537	346, 331, 303
Compound 5	18.96	2,591	346, 303, 247
Compound 6	19.58	2,679	344, 329, 301, 260, 137
(9R)-HHCP	19.68	2,692	344, 301, 260, 221
(9S)-HHCP	19.80	2,708	344, 301, 260, 221
CBP	20.88	2,835	338, 323, 238
CBDP	19.51	2,670	342, 327, 274, 221
Δ^9 -THCP	19.99	2,732	342, 327, 299, 259, 243

Note: Spectra are included in Supporting Information S60–S70.

Abbreviations: RRI, relative retention index (Kováts index); RT, Retention time.

configuration of the hydrogens at C6a and C10a. By comparison with (9R)- and (9S)-*cis*-HHC from the literature, it is observable that the according fragments were found. The fragments m/z 344, 301, and 221 are shifted by +28 due to the longer alkyl chain of compound 2 (+C₂H₄), and the fragment m/z 260 remains identical because this fragment ion results from the fragmentation of the alkyl chain.⁷

3.3.4 | Mass spectrum of compound 3

The isolated compound **3** is (9*R*)-HHCP. The same retention time and mass spectrum were obtained as from the reference compound.

3.3.5 | Mass spectrum of compound 4

Comparison of the mass spectrum of compound **4** with a mass spectrum from a similar molecule lacking the heptyl chain revealed that the main fragments are shifted by the mass of heptylene (C₇H₁₄, *m/z* 98). The relative abundances of the main peaks are similar to those reported in the literature.¹⁷ These fragment ions occur therefore from the fragmentation of the tricyclic moiety. The most abundant fragments are the molecular ion ([M]⁺, *m/z* 346), loss of a methyl radical ([M-CH₃]⁺, *m/z* 331), and loss of a propyl radical from the *gem*-dimethyl group ([M-C₃H₇]⁺, *m/z* 303, base peak). In addition, loss of a heptyl radical can also be observed ([M-C₇H₁₅]⁺, *m/z* 247). A mechanism for this reaction is shown in Figure 4.¹⁸

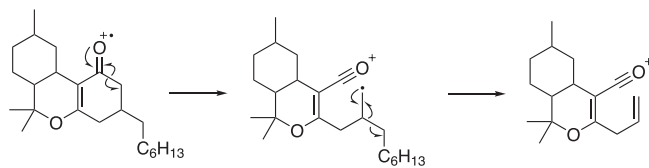


FIGURE 4 Fragmentation mechanism for the loss of a heptyl radical from compound **4**.

3.3.6 | Mass spectrum of compound 5

The same fragments appear as in compound **4** with *m/z* 303 as base peak. Slight changes in the abundances of the characteristic fragment ions are observed. The same fragmentation mechanisms can occur as in compound **4**.

3.4 | Chiral derivatization

Compounds **1–6** were derivatized in presence of the acylation catalyst DMAP with either (*R*)-MTPA-Cl or (*S*)-MTPA-Cl to their respective Mosher esters. A solution of (9*R*)-HHCP, (9*S*)-HHCP, or of one of the compounds **1–6** ($\gamma = 1$ mg/ml, 10 μ l, dry DCM) was evaporated to dryness. DMAP solution ($\gamma = 10$ mg/ml in dry DCM, 10 μ l), dry DCM (50 μ l), and either (*R*)-MTPA-Cl or (*S*)-MTPA-Cl solution ($\sigma = 10$ ml/l in dry DCM, 10 μ l) were added to the residue. The solutions were incubated at 50°C for 15 h overnight. The samples were evaporated to dryness, and the residue was dissolved in 50 μ l EtOAc and analyzed by GC-MS. An impure sample fraction containing (9*S*)-HHCP was derivatized with a similar protocol using 20 μ l of a sample solution ($\gamma = 1$ mg/ml) and 20 μ l (*R*)-MTPA-Cl or (*S*)-MTPA-Cl ($\sigma = 10$ ml/L). The Mosher esters of the isolated compounds and the references (9*R*)-HHCP and (9*S*)-HHCP are summarized in Table 6. (*S*)-MTPA esters are the products of derivatization with (*R*)-MTPA-Cl and vice versa.

The (*S*)-MTPA and (*R*)-MTPA esters of one enantiomer of compound **1** ((2*S*,5*R*,6*S*)-*iso*-HHCP) are the enantiomers of the (*R*)-MTPA and (*S*)-MTPA esters of the other enantiomer of compound

TABLE 6 Chromatographic data and relevant ions of the (*R*)- and (*S*)-MTPA esters of the isolated compounds and reference compounds.

Name	RT/min	RRI	ee	Relevant ions
(<i>S</i>)-MTPA ester of 1	24.58	3,131	72%	560, 475, 273, 189
(<i>S</i>)-MTPA ester of 1 *	25.00	3,127	-	560, 475, 273, 189
(<i>R</i>)-MTPA ester of 1	25.06	3,159	82%	560, 475, 273, 189
(<i>R</i>)-MTPA ester of 1 *	24.50	3,156	-	560, 475, 273, 189
(<i>S</i>)-MTPA ester of 2	24.81	3,145	100%	560, 517, 485, 327, 189
(<i>R</i>)-MTPA ester of 2	25.24	3,170	100%	560, 514, 485, 327, 189
(<i>S</i>)-MTPA ester of 3	26.25	3,224	100%	560, 517, 485, 327, 189
(<i>R</i>)-MTPA ester of 3	25.69	3,197	100%	560, 517, 485, 327, 189
(<i>S</i>)-MTPA ester of 6	30.04	3,387	100%	560, 517, 343, 315, 274, 189
(<i>R</i>)-MTPA ester of 6	30.08	3,389	100%	560, 517, 343, 315, 274, 189
(<i>S</i>)-MTPA ester of (9 <i>S</i>)-HHCP from sample	27.27	3,274	100%	560, 517, 485, 327, 189
(<i>S</i>)-MTPA ester of (9 <i>S</i>)-HHCP from sample	27.04	3,262	100%	560, 517, 485, 327, 189
(<i>S</i>)-MTPA ester of (9 <i>R</i>)-HHCP	26.30	3,227	100%	560, 517, 485, 327, 189
(<i>R</i>)-MTPA ester of (9 <i>R</i>)-HHCP	25.77	3,201	100%	560, 517, 485, 327, 189
(<i>S</i>)-MTPA ester of (9 <i>S</i>)-HHCP	27.43	3,281	100%	560, 517, 485, 327, 189
(<i>R</i>)-MTPA ester of (9 <i>S</i>)-HHCP	27.16	3,268	100%	560, 517, 485, 327, 189

Note: Spectra included in Supporting Information S73–S102. Enantiomeric excess was calculated from GC-MS area-% of the Mosher esters. Abbreviations: **1***, enantiomer of compound **1**; ee, enantiomeric excess; RRI, relative retention index (Kováts index); RT, retention time.

1 ((2*R*,5*S*,6*R*)-*iso*-HHCP). The enantiomeric Mosher esters have the same retention time (see Table 6). Relative intensities of the Mosher esters to each other are reversed when compound **1** is esterified with (*S*)-MTPA-Cl instead of (*R*)-MTPA-Cl. This indicates that compound **1** is a scalemic mixture. An enantiomeric excess of 72–82% was calculated from GC-MS area-%. The Mosher esters of both enantiomers of compound **1** are shown in Figure 5.

Chiral derivatization revealed that the epimers of HHCP in the sample were enantiopure. Comparison with reference standards showed that the HHCP epimers in the sample were indeed (9*R*)-HHCP and (9*S*)-HHCP and not their unnatural enantiomers ((6*aS*,9*S*,10*aR*)- and (6*aS*,9*S*,10*aS*)-HHCP).

3.5 | Mass spectra of high-molecular impurities

A fraction was collected that contained several compounds with molecular ions of *m/z* 480 and 482. Some molecules with a molecular ion of *m/z* 480 (base peak) showed the ions [M-15]⁺, [M-43]⁺, [M-84]⁺, and [M-123]⁺, indicating that similar fragments are generated as in HHCP. These compounds are sideproducts resulting from a second alkylation on the cyclic diketone. Fragmentation patterns are shown in Figure 6.

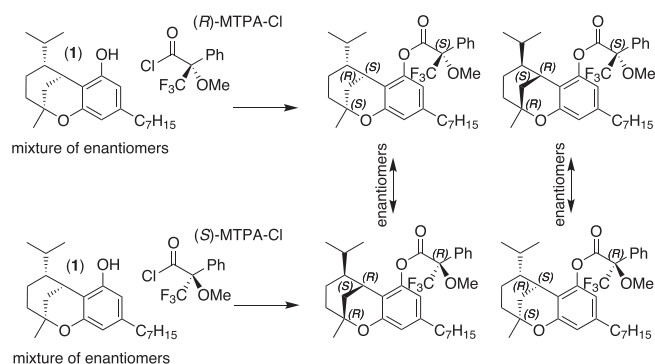


FIGURE 5 Formation of (*S*)-MTPA- (top) and (*R*)-MTPA esters (bottom) of compound **1** and its enantiomer. Two pairs of enantiomers are formed.

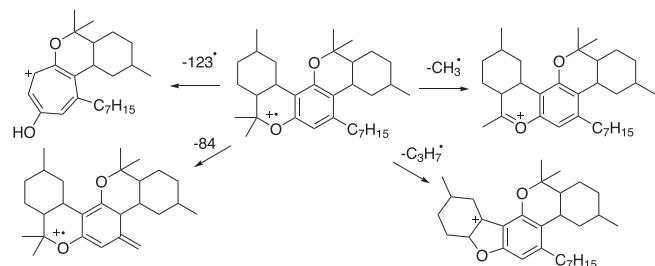


FIGURE 6 Fragmentation of the bisalkylated product shown on an *ortho,para*-disubstituted molecule.

Two different substitution patterns for the bisalkylation are plausible, which are shown in Figure 7. Each of the molecules possesses six stereogenic centers, which would lead to a total of 48 enantiomeric pairs and 4 *meso* compounds, explaining the crowded extracted ion chromatogram. It can be expected that the fragmentation patterns are similar.

In addition, bisalkylated *iso*-cannabinoids might also be formed. Some of the molecules with a molecular ion of *m/z* 480 show the fragments [M-15]⁺, [M-84]⁺, and [M-85]⁺, which are the same losses as observed for compound **1**. Substituted *iso*-HHCPs are therefore likely structures, which add even more complexity in the extracted ion chromatogram. They are shown in Figure 8.

Such bisalkylated compounds are known side products from the synthesis of other cannabinoids. Houry et al.^{19,20} described a double condensation product from the reaction of olivetol with limonene or α -pinene in the presence of phosphorous oxychloride. Millimaci et al.⁸ described that bis-addition can occur from the reaction of 4-isopropyl-1-methylcyclohex-2-en-1-ol with olivetol under acidic conditions. Similar observations were made from the synthesis of THC from olivetol with menthadienol under acidic conditions leading to a disubstituted olivetol.²¹

3.6 | Trimethylsilylation of the high-molecular weight fraction

The fraction, which contained the high-molecular weight impurities, was evaporated to dryness and dissolved in 500 μ l EtOAc. At 90°C, 100 μ l of this solution and 100 μ l MSTFA were incubated for 40 min. The solution was then evaporated to dryness and dissolved in 1 ml EtOAc; this was repeated without MSTFA. The samples were measured by GC-MS. The silylated sample showed peaks with molecular

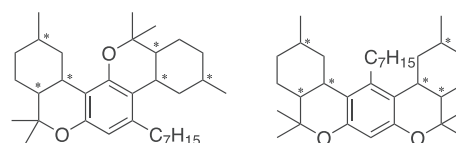


FIGURE 7 *o,p*-disubstitution pattern (left) and *o,o*-disubstitution pattern (right). Stereogenic centers are marked with an asterisk (*ortho*- and *para*- refer to the carbon-rest in relation to the position of the heptyl group).

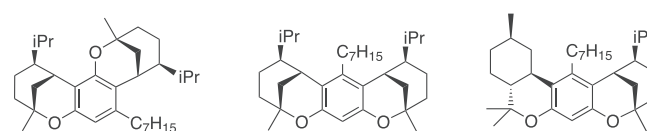


FIGURE 8 Examples of disubstituted bridged molecules. *o,p*-disubstitution (left) and *o,o*-disubstitution (mid) and a mixed form (right).

ions, which would fit to mono- and disilylation (m/z 554, 626). The extracted ion chromatograms of the derivatized and underivatized sample from m/z 480 were identical, indicating that these compounds do not have reactive groups (Supporting Information S105 and S106). The silylated molecules are possibly TMS-enol ethers of intermediates prior Hetero-Diels-Alder cyclization. An interesting ion of m/z 429 can be seen in the mass spectra of compounds with a molecular ion of m/z 554. This ion might result from the fragmentation of the citronellyl-sidechain; a mechanism is provided in Figure 9. The same loss of 125 can be seen in an underivatized sample with the ion m/z 482; this molecule is not present after derivatization with MSTFA (24.94 min). Some monoalkylated compounds with m/z 346 also show the acylium ion from the loss of 125 amu; the tricyclic ketones **4** and **5** do not.

3.7 | Potential synthetic route to HHCP and side products

The presence of the two α,β -unsaturated ketones **4** and **5** is a strong hint that this HHCP sample was synthesized from 5-heptylcyclohexa-1,3-dione. Knoevenagel condensation of this diketone with (*R*)-citronellal, subsequent Hetero-Diels-Alder reaction, and aromatization

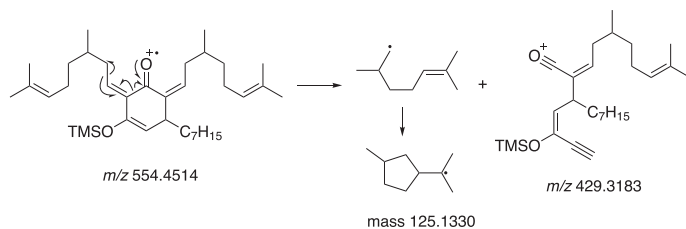


FIGURE 9 Fragmentation mechanism of the TMS-enol ether with an m/z 554 to the ion m/z 429.

leads to enantiopure (6*aR*,9*R*,10*aR*)-HHCP.²² An alternative aromatization to olivetol derivatives using catalytic amounts of iodine in dimethylsulfoxide was shown recently.²³ This sequence with citral A or B as aldehyde would lead to cannabichromephorol (CBCP) and not Δ^9 -THCP, since the 6π -electrocyclization would be the preferred pathway and not the Hetero-Diels-Alder reaction.²⁴ The presence of the so-called abnormal or *ortho* substitution pattern (compounds **5** and **6**), where the alkyl chain and the phenol or ketone change position might also be explained by this reaction sequence. The α,β -unsaturated ketones **4** and **5** are intermediates in this sequence and deliver the desired phenols after oxidation. A plausible pathway to the ketones **4** and **5** is shown in Figure 10.

The presence of *iso*-HHCP (compound **1**) can occur from cyclization of CBDP with the cyclic olefin and subsequent hydrogenation of the double bond (see Figure 11). Derivatization of compound **1** with (*R*)- and (*S*)-MTPA-Cl revealed that this compound is scalemic, which means that the precursor was scalemic as well, a mixture of (+)- and (–)-*trans*-CBDP for instance, therefore confirming that not a natural substance was used to synthesize this sample. Partial racemization seems unlikely due to lack of acidic protons at the stereogenic centers. It is not known how and if CBDP was formed in this process. CBDP was not detected in the sample.

Chiral derivatization revealed that the isolated phenols besides compound **1** were enantiopure. Compounds **2** and **3** are the *cis* and *trans* products of the intramolecular Hetero-Diels-Alder reaction of condensed (*R*)-citronellal (see Figure 12). Due to the diastereoselectivity of the reaction, the respective *trans*-product of (*S*)-citronellal should be (6*aS*,9*S*,10*aS*)-HHCP, the enantiomer of (9*R*)-HHCP.²² This product was not found. A chiral analysis of the impure fraction containing (9*S*)-HHCP revealed that this fraction contained only (9*S*)-HHCP and not its enantiomer (6*aS*,9*R*,10*aS*)-HHCP. The latter could have been a plausible side product if only (*R*)-citronellal was used to prepare this sample, as their stereochemistry at this position is identical.

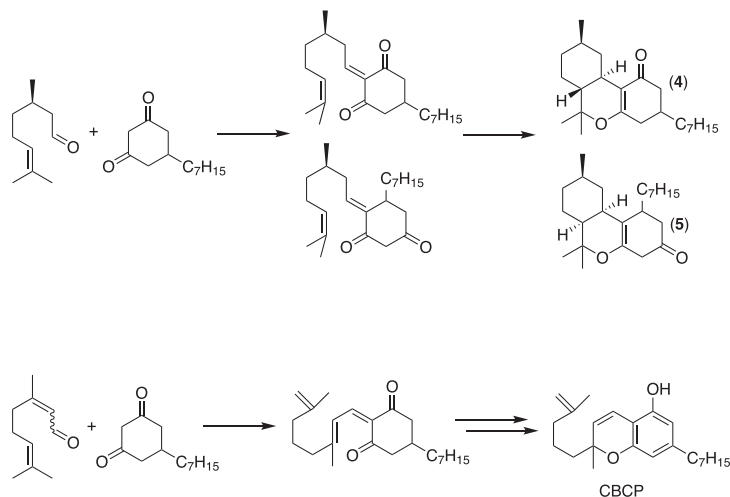


FIGURE 10 Top: plausible synthetic pathway to the α,β -unsaturated ketones **4** and **5** starting from (*R*)-citronellal. Bottom: same reaction pathway using *E*- or *Z*-citral as the aldehyde leads to CBCP.

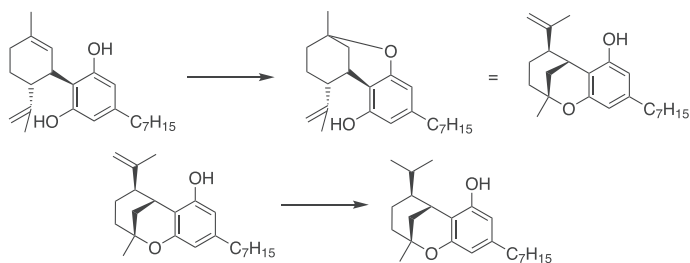


FIGURE 11 Cyclization of natural occurring (–)-*trans*-CBDP with subsequent hydrogenation to compound **1** would only deliver enantiopure (2*R*,5*S*,6*R*)-9-heptyl-5-isopropyl-2-methyl-3,4,5,6-tetrahydro-2*H*-2,6-methanobenzo[*b*]oxocin-7-ol.

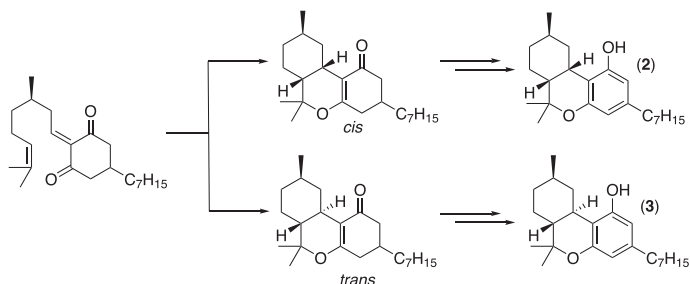


FIGURE 12 Plausible formation of compounds **2** and **3** ((9*R*)-HHCP) from the condensed (*R*)-citronellal adduct.

4 | CONCLUSIONS

The impurity profile and the isolated compounds from the analyzed HHCP sample lead to the conclusion that this sample was made synthetically. To the authors' knowledge, neither (9*R*)-HHCP nor (9*S*)-HHCP has yet been found in *Cannabis*. Disproportionation from naturally occurring Δ^9 -THCP is plausible, but the by-product of this reaction, cannabiphorol, was not found in the sample. It is not known for certain how this sample was prepared, but the sample contained unnatural stereoisomers (*cis*-HHCP), unnatural regioisomers (*abn*-HHCP), and higher condensed molecules similar to side products from the total synthesis of similar cannabinoids. The isolated ketones are most probably unreacted intermediates from chemical synthesis (precursors of (9*R*)-HHCP and *cis-abn*-HHCP) as they are not known to be intermediates from the cannabinoid biosynthesis. The chosen pathway allowed acceptable stereocontrol of the centers C6a and C10a. Most of the impurities in the sample could not be isolated in an acceptable purity for structure elucidation. Due to their fragmentation behavior, they are probably isomers of the isolated compounds. Unreacted starting material was not found, which makes it difficult to understand which synthetic route was chosen. It is very likely that this sample is a mixture of different synthetic batches from different synthetic routes. The presence of (9*S*)-HHCP cannot be explained by the proposed pathway, and the presence of ketones **4** and **5** cannot be explained by a pathway starting from an olivetol homolog. It is

assumed that not every manufacturer uses the same pathway to synthesize HHCP and similar compounds but CBD as starting material is certainly not one of these.

ACKNOWLEDGMENTS

Remo Arnold from the University of Bern is acknowledged for the help and material he provided for the column chromatography. Christian Bissig from the Forensic Institute of Zurich is acknowledged for the fruitful discussions concerning semisynthetic cannabinoids.

ORCID

Willi Schirmer <https://orcid.org/0009-0004-5579-2217>

Martina Vermathen <https://orcid.org/0000-0002-0796-1643>

Julien Furrer <https://orcid.org/0000-0003-2096-0618>

Stefan Schürch <https://orcid.org/0000-0001-5109-4623>

Wolfgang Weinmann <https://orcid.org/0000-0001-8659-1304>

REFERENCES

- Schweizerische Eidgenossenschaft. Verordnung des EDI über die Verzeichnisse der Betäubungsmittel, psychotropen Stoffe, Vorläuferstoffe und Hilfschemikalien (Betäubungsmittelverzeichnisverordnung, BetmVV-EDI) vom 30. Mai 2011 (Stand am 9. Oktober 2023), <https://www.fedlex.admin.ch/eli/cc/2011/363/de>
- Bueno J, Greenbaum EA. (–)-*trans*- Δ^9 -Tetrahydrocannabinophorol content of *Cannabis sativa* inflorescence from various chemotypes. *J. Nat. Prod.* 2021;84(2):531–536. doi:10.1021/acs.jnatprod.0c01034
- Citti C, Linciano P, Russo F, et al. A novel phytocannabinoid isolated from *Cannabis sativa* L. with an *in vivo* cannabimimetic activity higher than Δ^9 -tetrahydrocannabinol: Δ^9 -Tetrahydrocannabinophorol. *Sci. Rep.* 2019;9(1):20335. doi:10.1038/s41598-019-56785-1
- Tanaka R, Kikura-Hanajiri R. Identification of hexahydrocannabinol (HHC), dihydro-*iso*-tetrahydrocannabinol (dihydro-*iso*-THC) and hexahydrocannabinophorol (HHCP) in electronic cigarette cartridge products. *Forensic. Toxicol.* 2023;42(1):71–81. doi:10.1007/s11419-023-00667-9
- Sorensen TS. On the non-equivalence of isopropyl CH₃ nuclear magnetic resonance signals. *Can. J. Chem.* 1967;45(13):1585–1588. doi:10.1139/v67-256
- Tonelli AE, Schilling FC, Bovey FA. Conformational origin of the nonequivalent ¹³C NMR chemical shifts observed for the isopropyl methyl carbons in branched alkanes. *J. Am. Chem. Soc.* 1984;106(4):1157–1158. doi:10.1021/ja00316a079
- Arnone A, Merlini L, Servi S. Hashish: synthesis of (+)- Δ^4 -tetrahydrocannabinol. *Tetrahedron.* 1975;31(24):3093–3096. doi:10.1016/0040-4020(75)80154-2
- Millimaci AM, Trilles RV, McNeely JH, Brown LE, Beeler AB, Porco JA Jr. Synthesis of Neocannabinoids using controlled Friedel-Crafts reactions. *J. Org. Chem.* 2023;88(18):13135–13141. doi:10.1021/acs.joc.3c01362
- Gaoni Y, Mechoulam R. The *iso*-tetrahydrocannabinols. *Israel J. Chem.* 1968;6(5):679–690. doi:10.1002/ijch.196800086
- Inoue T, Inoue S, Sato K. Lewis acid catalyzed reaction of *o*-[1-(alkylthio)alkyl]phenols: the generation and reaction of *o*-quinonemethides and applications to cannabinoid synthesis. *Bull. Chem. Soc. Jpn.* 1990;63(6):1647–1652. doi:10.1246/bcsj.63.1647
- Vree TB. Mass spectrometry of cannabinoids. *J. Pharm. Sci.* 1977;66(10):1444–1450. doi:10.1002/jps.2600661025
- Harvey DJ, Brown NK. Electron impact-induced fragmentation of the trimethylsilyl derivatives of monohydroxy-hexahydrocannabinols. *Biol. Mass Spectrom.* 1991;20(5):292–302. doi:10.1002/bms.1200200510

13. Budzikiewicz H, Alpin RT, Lightner DA, Djerassi C, Mechoulam R, Gaoni Y. Massenspektroskopie und ihre Anwendung auf strukturelle und stereochemische Probleme—LXVIII: Massenspektroskopische Untersuchung der Inhaltstoffe von Haschisch. *Tetrahedron*. 1965; 21(7):1881-1888. doi:10.1016/S0040-4020(01)98657-0
14. Kováts E. Gas-chromatographische Charakterisierung organischer Verbindungen. Teil 1: Retentionsindices aliphatischer Halogenide, Alkohole, Aldehyde und Ketone. *Helv. Chim. Acta*. 1958;41(7):1915-1932. doi:10.1002/hlca.19580410703
15. van den Dool H, Kratz PD. A generalization of the retention index system including linear temperature programmed gas-liquid partition chromatography. *J. Chromatogr. A*. 1963;11:463-471. doi:10.1016/S0021-9673(01)80947-X
16. Terlouw JK, Heerma W, Burgers PC, et al. The use of metastable ion characteristics for the determination of ion structures of some isomeric cannabinoids. *Tetrahedron*. 1974;30(23-24):4243-4248. doi:10.1016/S0040-4020(01)97415-0
17. Fernandes S, Rajakannu P, Bhat SV. Efficient catalyst for tandem solvent free enantioselective Knoevenagel-formal [3+3] cycloaddition and Knoevenagel-hetero-Diels-Alder reactions. *RSC Adv*. 2015;5(83): 67706-67711. doi:10.1039/C5RA09865C
18. Vandewalle M, Schamp N, de Wilde H. Studies in organic mass spectrometry III 1, 3-cyclohexanediones. *Bull. Soc. Chimiques Belg*. 1967; 76(1-2):111-122. doi:10.1002/bscb.19670760112
19. Houry S, Mechoulam R, Fowler PJ, Macko E, Loev B. Benzoxocin and benzoxonin derivatives. Novel groups of terpenophenols with central nervous system activity. *J. Med. Chem*. 1974;17(3):287-293. doi:10.1021/jm00249a006
20. Houry S, Mechoulam R, Loev B. Benzoxocin and benzoxonin derivatives. Novel groups of terpenophenols with central nervous system activity. *Correction J. Med. Chem*. 1975;18(9):951-952. doi:10.1021/jm00243a020
21. Petrzilka T. Chemie synthetischer hanfderivate. *B Schweiz Akad. Med*. 1971;27. doi:10.5169/seals-307854
22. Tietze LF, von Kiedrowski G, Berger B. Stereo- and Regioselective synthesis of enantiomerically pure (+)- and (-)-Hexahydrocannabinol by intramolecular cycloaddition. *Angew. Chem. Int. Ed. Engl*. 1982; 21(3):221-222. doi:10.1002/anie.198202212
23. Hurem D, Macphail BJ, Carlini R, Lewis J, McNulty J. A catalytic, oxidative synthesis of olivetol, methyl olivetolate and orthogonally protected methyl ether derivatives. *SynOpen*. 2021;5(1):86-90. doi:10.1055/a-1440-9732
24. Tietze LF, Kiedrowski GV, Berger B. A new method of aromatization of cyclohexenone derivatives; synthesis of cannabichromene. *Synthesis*. 1982;1982(8):683-684. doi:10.1055/s-1982-29902

SUPPORTING INFORMATION

Additional supporting information can be found online in the Supporting Information section at the end of this article.

How to cite this article: Schirmer W, Gjuroski I, Vermathen M, Furrer J, Schürch S, Weinmann W. Isolation and characterization of synthesis intermediates and side products in hexahydrocannabinophorol. *Drug Test Anal*. 2024;1-13. doi:10.1002/dta.3759